# STEEL GRIPS

JOURNAL OF STEEL AND RELATED MATERIALS

www.steel-grips.com

## Products

GRIPS media GmbH

ISSN 1611-4442

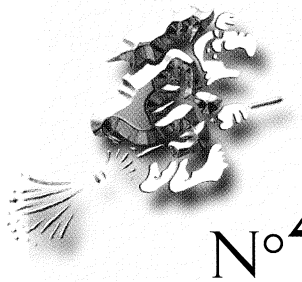

N°4

JULY/AUGUST 2005

*Christof Sommitsch, Michael Walter, Siegfried Kleber, Peter Pölt and Stefan Mitsche:*

# On the determination of the recrystallised fraction during hot forming

Recrystallisation during hot forming processes is a decisive process for formability and control of the microstructure. Forming processes can be optimized by the simulation of grain structure development. The relevant computational models need material parameters, which are essentially determined by laboratory experiments. This includes determination of recrystallised fractions and grain size development. Direct and indirect methods exist for the analysis of the grain structure. First tries to determine the softening by relaxation measurements or by the comparison from multi-step sequential deformations. The latter consists of the metallographical investigation of a two-dimensional cross-section by methods of light microscopy and automatic image analysis or with the help of electron microscopy and grain orientation analysis. In consequence different methods are compared by means of the nickel base alloy Alloy 80A.

Hot forming processes of metallic materials experience dynamic and static softening mechanisms, in order to achieve large strains. With processes that need a multiple deformation, one tries to remain in the optimum forming window by the correct choice of the deformation parameters (e.g. hot forging). Very large work pieces and complex, difficult to deform materials require intermediate annealing in order to gain an optimum forming temperature (e.g. open-die forging of nickel basis alloys). This forming window refers to the temperature and the deformation rate, with which the workability conforms to the characteristic values of the machine. In addition the formability of the material must be ensured. The formability as a function of temperature and strain rate is represented in processing maps for different materials [1...2]. These maps are based on the consideration into which portions the generated deformation energy dissipates in strengthening and softening.

**Table 1:** Chemical composition of the Alloy 80A, mass contents in %

| C | Si | Mn | Cr | Mo | Ni | Co | Ti | Al |
|---|---|---|---|---|---|---|---|---|
| 0.06 | 0.15 | 0.04 | 19.6 | 0.03 | 75.1 | 0.06 | 2.52 | 1.67 |

Here, apart from the crystallographic slip ability and the affinity of the material for recrystallisation, also thermodynamic processes like precipitation and/or the dissolution of particles play a relevant role.

A further important aspect in hot forming lies in the possible generation of a microstructure with optimized mechanical properties. In case of thermo-mechanical rolling, for example, by adjusting the process conditions at the final sizing pass, a matrix transformation that is adjusted to the subsequent processing of the rolled material and thus optimized mechanical properties are reached [3].

Optimization of the forming process in view of adjusting to a desired microstructure requires the employment of process simulation with the help of the finite difference and/or finite element method. Development of the grain structure as a function of the process conditions can be described by implementing structure models. These models need material parameters as input for modelling of the flow behaviour, grain growth and recrystallisation. Dynamic, meta-dynamic and static recrystallisation are relevant softening mechanisms for alloys with relatively low stacking fault energy (e.g. austenitic steels, nickel base alloys, copper). The description of these mechanisms requires advanced analysis methods and computation models. In further consequence some examples are specified here.

## Methods

**Indirect analysis methods.** Indirect methods examine the grain structure by means of interactions of the material with waves of different kinds. This work deals with light and electron microscopic procedures in greater detail as well as different practices, for instance the laser ultrasonic technique exist, with which continuously and non-destructively primary recrystallisation is observed [4]. A new three-dimensional procedure for the description of the grain structure development is based on the micron-resolution X-ray Laue diffraction [5].

*Experimental program.* The following investigations [6] have been accomplished on compressed specimens of the Alloy 80A with the chemical composition given in **table 1.**

For the following recrystallisation analysis, upset tests at a temperature of 1120 °C and a deformation rate of 0.1 $s^{-1}$ for 19 different true strains of 0.105... 1.03 have been performed using a Gleeble-3800 Hydro Wedge system. The cylindrical samples (Ø 10 · 12 $mm^2$) originate from a rolled round bar and exhibited a homogeneous and fine-grained structure. The samples were heated up conductively to 1220 °C, held at constant temperature for 60 s and cooled down to a deformation temperature of 1120 °C. The mean grain size of the initial structure created in such a way was 120 µm.

The deformed samples were prepared in longitudinal and transversal directions. While the longitudinal section origi-

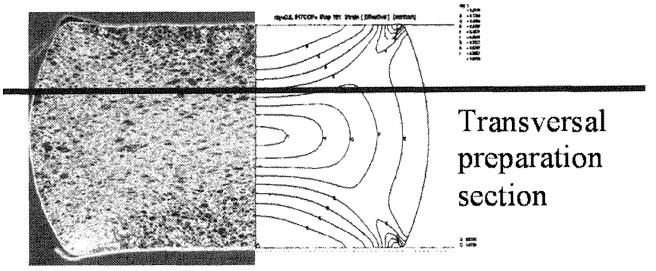


**Fig. 1:** Macro view of the longitudinal section combined with the distribution of effective strains that were calculated by the FEM

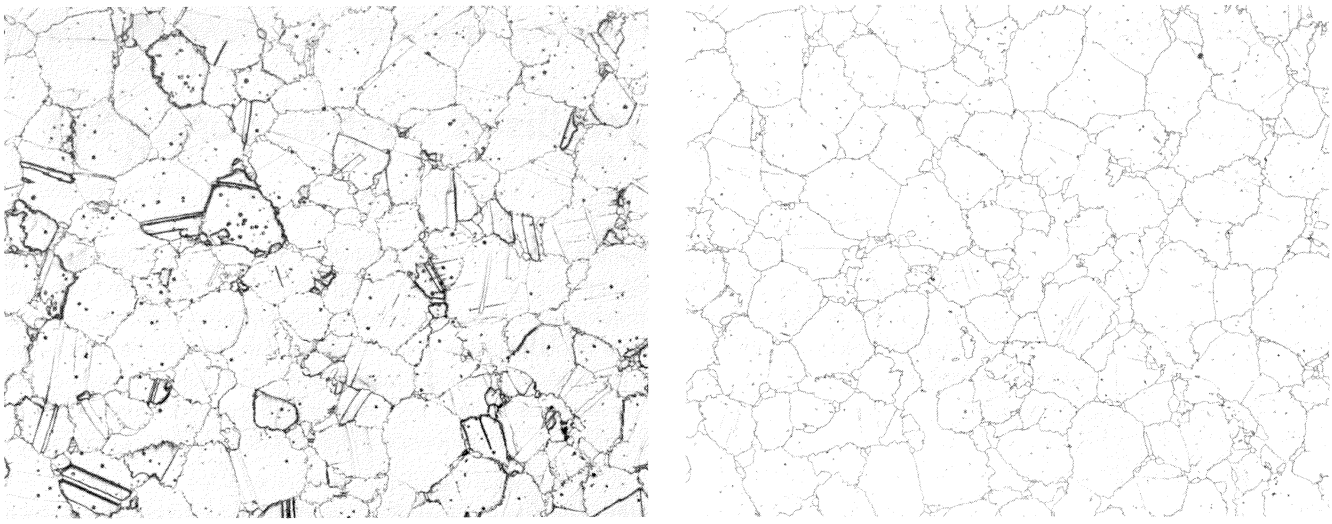

**Fig. 2:** Classical etching (a) and electrolytic etching (b) by comparison (Alloy 80A)

nates from the centre of the sample, the transversal section was extracted from a position which ensured that the local strain rate corresponds to the global strain rate in the sample. This position was determined by FEM calculations, **fig. 1**.

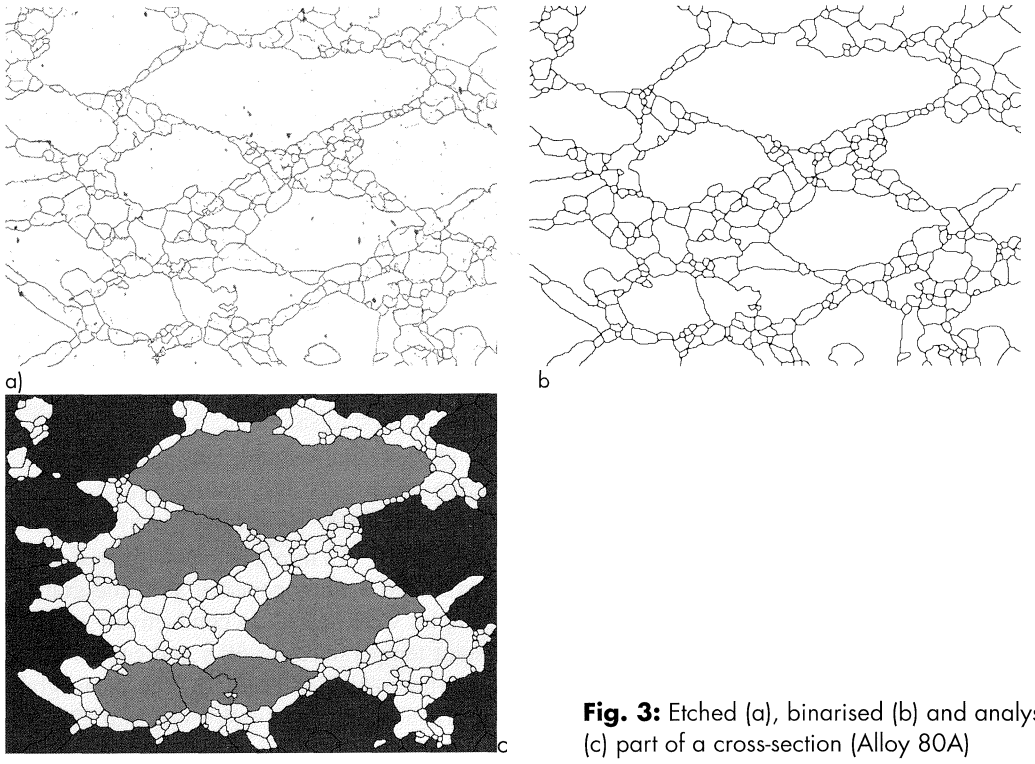


**Fig. 3:** Etched (a), binarised (b) and analysed (c) part of a cross-section (Alloy 80A)

*Light microscopy (LIMI) and automatic image analysis.* For the light microscopic investigations, samples were embedded, ground and polished with dispersions [6]. The classical etching for this alloy (50 ml $H_2O$, 50 ml ethanol, 50 ml HCl, 10 g $CuSO_4$) supplies a meaningful structure representation for the qualitative view, **fig. 2a**. However, it is not suitable for a quantitative, image analytical procedure due to a similar representation of twin and grain boundaries. With the help of electrolytic etching on the basis of glycerol and hydrofluoric acid it has been attained to suppress twin etching and thus ensure a homogeneous etching of the grain boundaries, **figs. 2b, 3a**.

The exposure of the pictures took place with the image analysis program ImageC. The pictures were directly binarised, **fig. 3b,** with the help of a further developed macro program, which additionally used several filters and evaluation programs of the software. That is necessary, in order to adjust arising variations of the image quality. The reconstruction of grain boundaries implies both the closing of interrupted boundaries as well as the handling of not attributable punctual entities. The binarised image is projected as an overlay on the original picture and examined by the user for its complete structural significance. If there are no salient maximum or minimum deviations, it is stored.

The analysis of the binarised images took place with the program Quant, whereby in contrast to classical structure analysis, no point or line intersection procedure, but a contour tracking procedure was used here, **fig. 3c**. To assign a grain to the deformed or recrystallised status, only pure geometrical characteristics are disposable. A critical grain size is suitable, for it is valid only as long as the recrystallised grains are smaller than the grains of the initial structure. Otherwise no significant cut-off point in the frequency distribution of the grains exists. As a distinction criterion, for each grain the deviation from the optimum circumference/area relationship, i.e. the quotient of the diameters of a coextensive circle and a circumference-equal circle was selected. A newly formed grain has accordingly a smaller quotient than

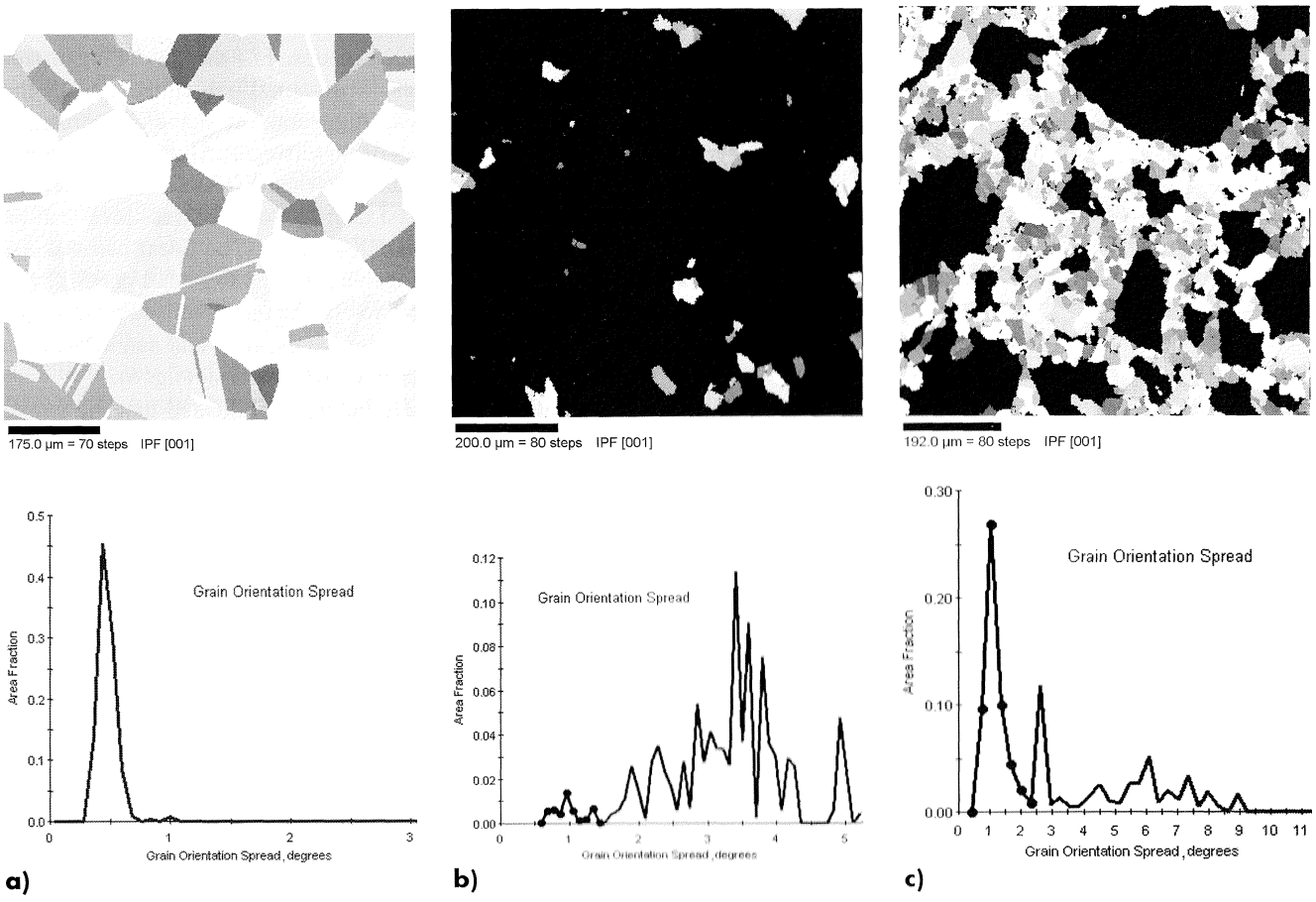


**Fig. 4:** Grain orientation map and grain orientation spread of both un-strained and strained samples (Alloy 80A, strain of 0.105 and 0.303, respectively). In (b-c), the deformed unrecrystallised grains are represented in black, whereas (a) shows the initially fully recrystallised structure. Different grey tones designate different grain orientations

a deformed grain that can be distinguished from the recrystallised grains. A meaningful threshold for the distinction between recrystallised and distorted grains resulted in a value of 0.125.

After classification of the grains into their respective recrystallisation class the recrystallised fraction and the grain size distribution of the recrystallised as well as the not recrystallised fractions were determined.

*Electron microscopy and electron backscatter diffraction* (*EBSD*). By the analysis of backscattered electrons, crystal orientations can be measured (OIM - orientation imaging microscopy). With the orientation imaging system, grains are separated due to their orientation difference. Apart from the results of conventional measurements at ambient temperature, presented here, there is special equipment, which permits in situ analysis of the primary static recrystallisation at higher temperatures [7...8].

A possibility to distinguish between recrystallised and deformed grains exists in the measurement of the deformation influenced misorientation in each grain [9]. The distinction is based on the grain orientation spread. If the latter is relatively small over the grain area, a recrystallised grain exists. The orientation spread of a fully recrystallised undeformed specimen resulted in approx. 0.5°, **fig. 4a**. In **fig. 4** also examples for true strains of 0.105 (fig. 4b) and 0.50 (fig. 4c), respectively, and the selected orientation spread thresholds are presented. The thresholds for the distinction between recrystallised and deformed grains for all analysed strains resulted in the range of 1 - 2 °. With increasing deformation also the critical orientation spread of recrystallised and deformed grains increases, since the already recrystallised grains are deformed concurrently, before they recrystallise again after reaching a critical strain. This continuous recrystallisation of already recrystallised grains during hot forming ends in a stationary behaviour.

**Direct analysis methods.** Apart from the very time-consuming indirect analysis methods, there has been the attempt to use direct measuring methods, which do not need microscopic investigations. For the determination of dynamic recrystallisation, flow curve sets can be analysed. With stress relaxation a reduction of the stored deformation energy is observed after deformation, as the anvil positions are kept constant. Alternatively, after a certain holding time the specimen is strained again and the two flow curves are compared (double hit compression test).

*Flow curve analysis.* For the determination of dynamic recrystallisation kinetics, temperature and deformation rate dependent flow curves can be analysed, in order to adapt semi-empirical grain structure models [10...12]. These models use equations of the Avrami type and describe the development of the grain structure as a function of temperature, deformation, deformation rate and grain size. The determination of the model parameters usually takes place by means of compression tests on servo-hydraulic test equipment. With higher deformation rates the transforma-

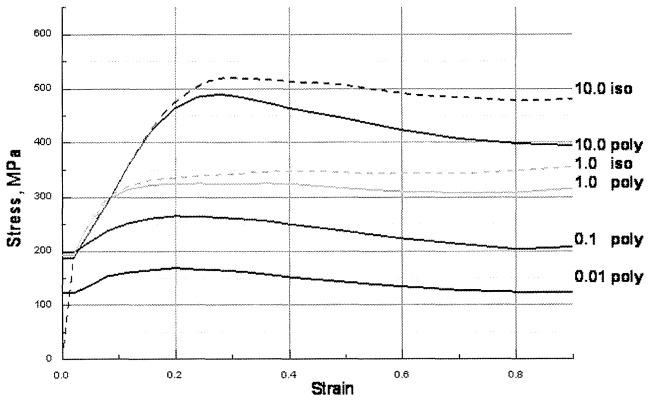


**Fig. 5:** Comparison of polytrope (measured) and isothermal flow curves for Alloy 80A at $T$ = 1000 °C

tion heat cannot be dissipated sufficiently any longer during the lab test, so that no isothermal conditions are obtained. However, the measured polytrope flow curves can be converted into isothermal curves by knowing the thermo-physical material properties, **fig. 5**. The determination of the relevant model parameters takes place by means of non-linear multiple regression on the basis of isothermal flow curves and the model equations.

*Stress relaxation and double hit compression test.* These techniques are suitable for the prediction of the meta-dynamic (MDRX) and static recrystallised (SRX) fractions. After a deformation step, temperature is kept constant in order to examine the ongoing softening process. With the stress relaxation test, tool position is kept constant and the stress drop is measured continuously [13]. On the other hand, with the double hit compression test, the sample is compressed again after a selected holding time at the same temperature, in order to be able to compare the flow curves [14]. With full recrystallisation and/or recovery, both curves must be congruent. If no softening occurs, the second flow curve continues directly from the point of the first unloading. Hence, the double hit compression test requires a multiple of trials in comparison to the stress relaxation test, since the recrystallisation rate must be illustrated by several test points. A further problem arises at higher deformation rates, when the samples differ in temperature during the two deformation hits, thus the latter aren't any longer directly comparable. For the used test equipment and alloy the critical deformation rate for isothermal conditions resulted in approx. 1 $s^{-1}$.

In the following, results are shown for the nickel basis alloy Alloy 80A [15]. The compression tests were performed with a Gleeble 3800 testing system for different temperatures (950 - 1200 °C). For the investigation of the MDRX the deformation rate was varied, whereas for the SRX analysis the pre-strain was altered. The pre-strain was set to twice the peak strain for the MDRX tests in order to guarantee stationary conditions, as well as to strain values below that for the investigation of the SRX kinetics. For the modelling of recrystallisation kinetics, semi-empirical equations of the Avrami type were used. In general, the shape of a stress relaxation curve consists of three stages, **fig. 6**. On the logarithmic scale, linear parts represent stress relaxation due to recovery, whereas a fast decrease of the stress level can be ascribed to SRX or MDRX kinetics. The linear parts can be easily described by tangents (60-15.3 *log t* and/or 95-27 *log t* in fig. 6), thus the fraction of the recrystallised matrix $X_{rxx}$ can be calculated by a rule of mixtures and can afterwards be fitted by an Avrami equation ($X_{Avrami}$) (fig. 6).

Evaluations of the stroke signal indicated that the stroke target could not be reached exactly due to the natural leakage rate of the big valve. Therefore, the servo-hydraulic system causes an additional stress release and the compression die moves measurably into the direction of unloading.

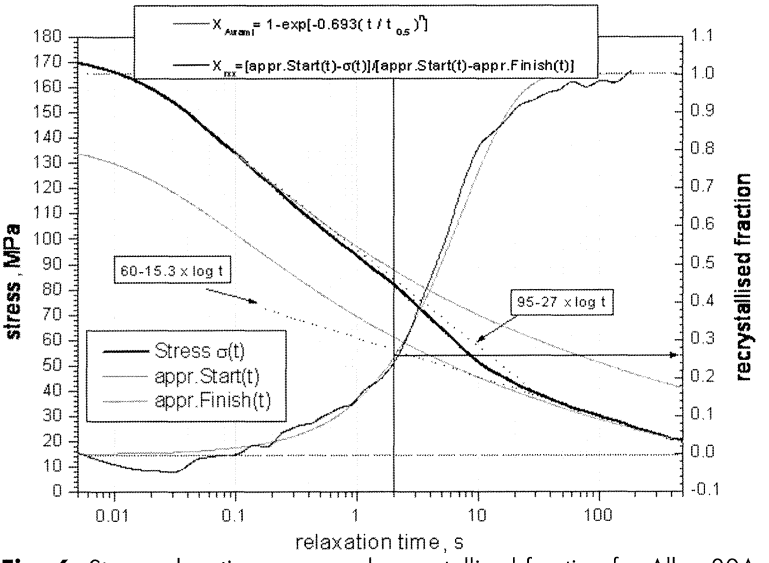


**Fig. 6:** Stress relaxation curve and recrystallised fraction for Alloy 80A at $T$ = 1050 °C, $\dot{\varepsilon}$ = 0.1 $s^{-1}$ and $\varepsilon = 0.7\varepsilon_{peak}$ ($\varepsilon_{peak}$: true strain at maximum stress, appr.Start and appr.Finish: approximative start and finish of recrystallisation)

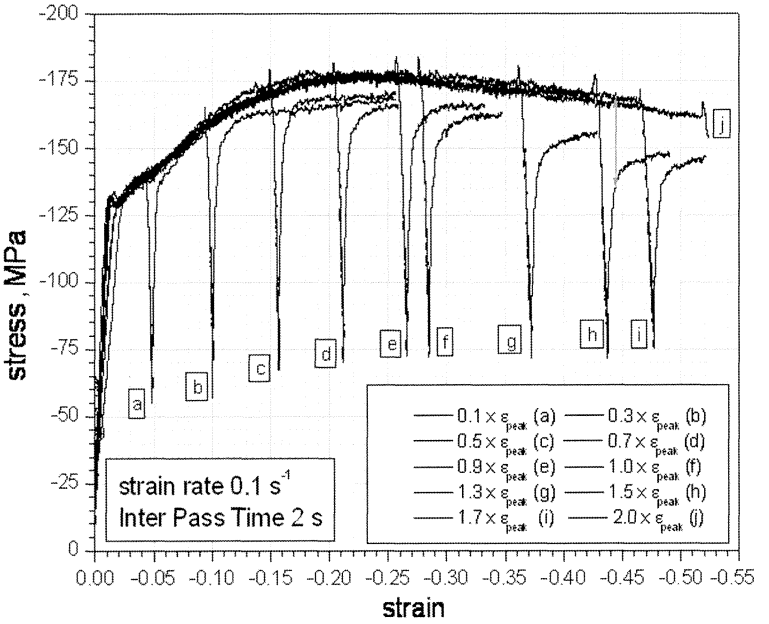


**Fig. 7:** Superposition of stress-strain curves for a series of double hit compression tests. The curves (a-j) represent different pre-strains

For this reason, specimens were charged by a very small strain during relaxation.

To validate the applied stress relaxation method, a series of double hit tests with constant pre-strains has been carried out. The interval time was set to 2 s. **Fig. 7** depicts the stress-strain history and shows the increasing softening with increasing pre-strain (SRX). If the pre-strains are high enough to produce steady state dynamic recrystallisation, saturation of the softening will occur.

A comparison of the double hit test and the stress relaxation method is illustrated in **fig. 8** and demonstrates that the double hit test leads to slightly higher fractions of recrystallisation. A reason for this could be the difference in microstructure in the first and second deformation hit. **Fig. 9** shows obtained Avrami plots for different strain rates at a constant pre-strain and temperature, respectively.

**Physically based microstructure models.** Beside the semi-empirical grain structure models, mentioned above, physical approaches are able to describe the microstructure evolution during hot forming more exactly. As an example

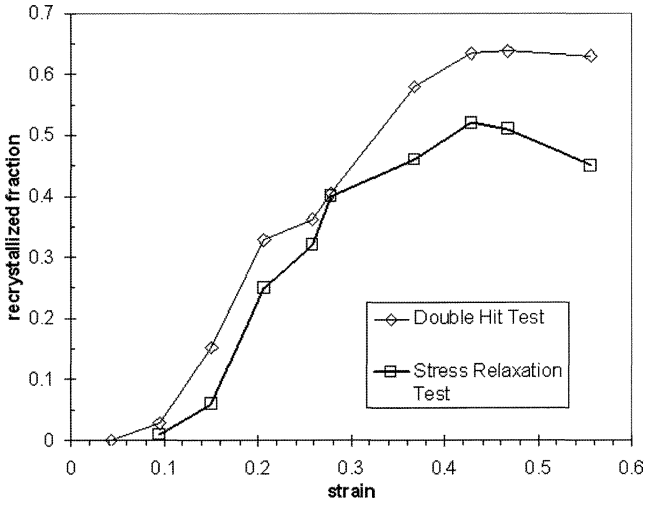


**Fig. 8:** Comparison of the stress relaxation test and the double hit compression test in reference to the recrystallised fraction (Alloy 80A) with $T$ = 1050 °C, $\dot{\varepsilon}$ = 0.1 $s^{-1}$ and a holding time of 2 s

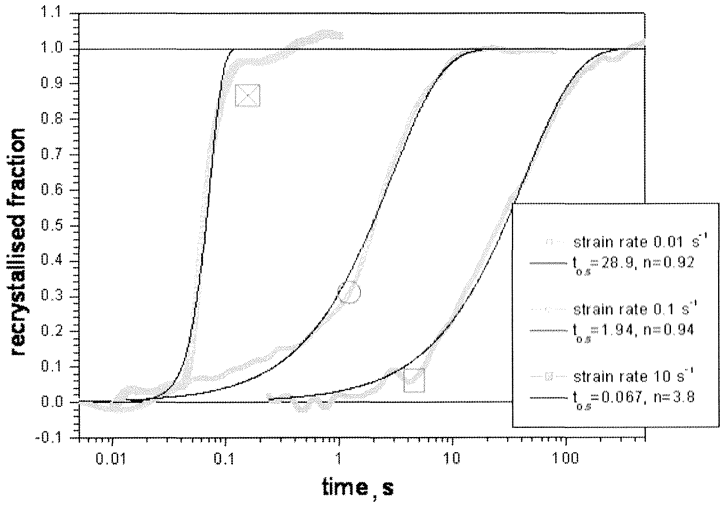


**Fig. 9:** Avrami plots of metadynamic recrystalllised kinetics of Alloy 80A for $T$ = 1050 °C, $\dot{\varepsilon}$ = 0.01, 0.1 and 10 $s^{-1}$

a model is reviewed in the following that refers recrystallisation and flow to the local dislocation density [16...20]. The dislocation density rate as a function of strain hardening and dynamic softening follows the equation

$$\frac{d\rho}{dt} = \frac{\dot{\varepsilon}}{\boldsymbol{b}\ l} - 2M\tau\rho^2 \qquad (1)$$

where $\dot{\varepsilon}$ is the strain rate, $\boldsymbol{b}$ the Burgers vector, $l$ the mean free path of the dislocations, $M$ the mobility of recovery and $\tau$ the average energy per unit length of a dislocation.

A critical dislocation density is necessary in order to initiate dynamic recrystallisation. The nucleus usually forms at pre-existing grain boundaries in the material, at least at higher strain rates. For an area that has just been recrystallised it is assumed that the dislocation density $\rho$ generated by the preceding strain is reduced to a very low value. The free energy difference that is deduced from the nucleation theory is maximized to find the critical conditions for the onset of dynamic recrystallisation (critical dislocation density $\rho_{cr}$ and critical nucleus radius).

For the examined alloys, the rate of nucleation is lower than the rate of growth by about four orders of magnitude and therefore controls the dynamic recrystallisation process. Due to the relatively low stacking fault energies of nickel base alloys as well as of austenitic steels at high temperatures, nucleation (i.e. the formation of high angle grain boundaries) is governed by thermal recovery based on the climb of edge dislocations with the rate of interface formation:

$$R_F = \frac{\dot{\varepsilon}\ P_R}{\boldsymbol{b}\ l} \qquad (2)$$

where $P_R$ is the probability of recovery of dislocations, leading to nucleation, and $R_F$ is the rate of interface formation.

With the assumption that nuclei predominantly form at the boundaries of the deformed grains with diameter $d_0$, the number of nuclei $Z$ can be calculated by:

$$Z(t) = \int Z'(t)\left[1 - f(t)\right]dt$$

$$= \int \frac{R_F}{N_d\ d_0}\left[1 - f(t)\right]dt \qquad (3)$$

where $Z'$ is the nucleation rate per volume, $N_d = A_{cr}/l_{cr}^2$ is the number of dislocations per critical nucleus, $A_{cr}$ is the cross-section of a critical nucleus and $l_{cr}$ is the mean free path of dislocations with a critical density ($l_{cr} \sim \rho_{cr}^{-1/2}$). In order to consider the decreasing area of potential nuclei formation with the ongoing recrystallisation, the nucleation rate is multiplied by ($1 - f$).

The recrystallised fraction $f(t_b)$ at the time $t_b$ is given by the sum of all grain volumes over all nucleation times $t_g$:

$$f(t_b) = \frac{\pi}{6}\int_{t_{cr}}^{t_b} D^3(t_g, t_b)\, Z'(t_g)\left[1 - f(t_g)\right]dt_g \qquad (4)$$

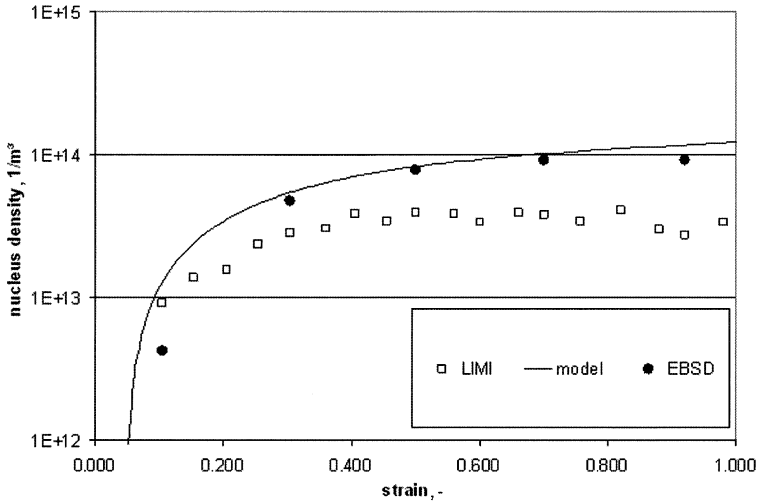


**Fig. 10:** Comparison of the nucleus density between experiments (EBSD and LIMI) and calculations of Alloy 80A at a temperature of 1120 °C and a deformation rate of 0.1 $s^{-1}$

where $D(t_g,t_b)$ is the size of a grain class, nucleated at the time $t_g$ and $Z'(t_g)\,dt_g$ is the grain number per class, which nucleated in the time interval $[t_g, t_g + dt_g]$.

**Figs. 10** and **11** show a comparison between the computational model and measurements by means of EBSD and LIMI concerning the development of the number of grains per unit volume as well as the recrystallised fraction. The recrystallised fractions determined by means of LIMI agree quite well up to approximately 60 % recrystallisation with the EBSD data and the calculated values. With higher recrystallisation fractions, LIMI measurement can not exactly differentiate between deformed and recrystallised grains with the described distinction criterion. Nevertheless, LIMI investigation with automated image analysis is a good instrument for the description of the grain structure development as a function of recrystallisation and grain growth. Two-dimensional investigation methods in general suffer from the disadvantage of a very much limited analysis field. Therefore, these metallographic methods in 2D are certainly not optimum tools for the investigation of nucleation and the very early stages of recrystallisation with its relatively small nucleus density.

## Conclusion

In this work different methods of the determination of the recrystallised fraction during hot forming processes have been described and compared. Both dynamic recrystallisation during hot forming and meta-dynamic as well as static recrystallisation after the forming pass can be described well by appropriate tools. For the direct investigation methods, the flow curve analysis in connection with semi-empirical grain structure models of the Avrami type for the description of dynamic recrystallisation has been illustrated. Here, isothermal flow curves are an important prerequisite, which, for high deformation rates and therefore rather adiabatic conditions can only be attained by reverse calculations. For the analysis of meta-dynamic and static recrystallisation, both the stress relaxation test and the double hit compression test are available. For the determination of recrystallisation kinetics, only one experiment per temperature and deformation rate is necessary with the stress relaxation test. However, problems often arise here both in holding the total strain constant during stress relaxation, in particular with servo-hydraulic aggregates, as well as in the separation of recovery and recrystallisation mechanisms. With the double hit compression test more experiments have to be accomplished in order to represent recrystallisation kinetics (3 - 5 points for the prediction of the Avrami curve). A further problem consists here in the fact that during the first and second hit, the grain structure as well as at higher deformation rates the temperature can be different. For the indirect measurement methods, light and electron microscopic examination methods have been illuminated as an example. An automated recrystallisation analysis of micrographs showed quite a good agreement with other procedures up to approximately 60 % recrystallised fraction. Beyond that the introduced distinction criterion between recrystallised and deformed - the deviation from the optimal circumference/area relationship of the grain - seems no longer meaningfully applicable. The EBSD method with the analysis of the grain orientation spread is a very purposive, although complex means for the description of the grain structure development. A physical grain structure model as an example of a theoretical calculation method has been presented briefly and compared with the measurements.

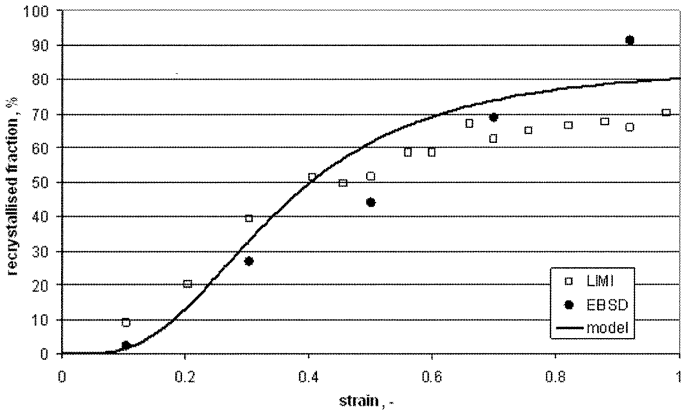


**Fig. 11:** Comparison of the recrystallised fraction between experiments (EBSD and LIMI) and calculations of Alloy 80A at a temperature of 1120 °C and a deformation rate of 0.1 $s^{-1}$

## References

[1] Kleber, S.; Walter, M.: Mater. Sci. Forum 426-432 (2003), p. 4173/78.
[2] Srinivasan, N.; Prasad, Y.: Met. Mater. Trans. 25A (1994), p. 2275/84.
[3] Buchmayr, B.: Mater. Sci. Forum 414-415 (2003), p. 377/84.
[4] Lindth-Ulmgren, E. et al.: Mater. Sci. Forum 467-470 (2004), p. 1353/62.
[5] Budai, J. et al.: Mater. Sci. Forum 467-470 (2004), p. 1373/78.
[6] Walter, M. et al.: Systematische Bestimmung des rekristallisierten Gefügeanteiles einer Nickelbasislegierung in Abhängigkeit vom Verformungsgrad, Proc. 37. Metallographie-Tagung 2003, September 17-19, 2003, Berlin.

[7] Fielden, I.; Rodenburg, J.: Mater. Sci. Forum 467-470 (2004), p. 1385/88.
[8] Nowell, M. et al.: Mater. Sci. Forum 467-470 (2004), p. 1401/06.
[9] Pölt, P. et al.: EBSD – and the recrystallisation of Ni-base-alloys, [in:] Proc. 13th Europ. Microscopy Congr., August 22-27, 2004, Antwerp, Vol. II, p. 695/96, D. Schryvers and J.-P. Timmermans [eds.:], Belgian Society for Electron Microscopy.
[10] Karhausen, K.: Integrierte Prozeß- und Gefügesimulation bei der Warmumformung, Umformtechn. Schrift., Bd. 52, Verlag Stahleisen, Düsseldorf, 1995.
[11] Sommitsch, C. et al.: BHMAM 146 (2001) No. 1, p. 6/9.
[12] Laasraoui, A; Jonas, J.J.: Metallurg. Trans. 22A (1991), p. 1545/57.
[13] Karjalainen, L.; Perttula, J.: ISIJ 36 (1996), p. 729/36.
[14] Djaic, R. A. P.; Jonas, J.J.: Journ. Iron Steel Inst. (1972) No. 4, p. 256/61.
[15] Kleber, S.; Sommitsch, C.: Mater. Sci. Forum 467-470 (2004), p. 1237/42.
[16] Sommitsch, C. et al.: Mater. Sci. Forum 426-432 (2003), p. 743/48.
[17] Sommitsch, C.: Theorie und Modell der mikrostrukturellen Entwicklung von Nickel-Basis-Legierungen während des Warmwalzens, Graz, 1999 (Dr. techn. thesis).
[18] Sommitsch, C.; Mitter, W.; Kleber, S.: Proc. Intern. Congr. on Advanced Materials, their Processes and Applications, Munich, September 25-28, 2000, Werkstoffwoche-Partnerschaft GbRmbH.
[19] Sommitsch, C.; Wieser, V.: Proc. 7th Europ. Conf. on Advanced Materials and Processes, Rimini, June 11-14, 2001, Associazione Italiana di Metallurgia.
[20] Sommitsch, C.; Wieser, V.; Kleber, S.: J. Mater. Proc. Techn. 125-126 (2002), p. 130/37.

Dr. Christof Sommitsch
Chair of Metal Forming
University of Leoben
Leoben

Dipl.-Ing. Michael Walter
Dr. Siegfried Kleber
Research and Development
Böhler Edelstahl GmbH
Kapfenberg

Dr. Peter Pölt
Institute for Electron Microscopy
Graz University of Technology
Graz

Austria